ACTIVE HEAD ROTATIONS AND EYE-HEAD COORDINATION*

Wolfgang H. Zangemeister† and Lawrence Stark

374: 540 – 559 (1981)

Reprinted from
ANNALS OF THE NEW YORK ACADEMY OF SCIENCES

ACTIVE HEAD ROTATIONS AND EYE-HEAD COORDINATION*

Wolfgang H. Zangemeister† and Lawrence Stark

Departments of Physiological Optics, Neurology, and Bioengineering
University of California
Berkeley, California 94720

INTRODUCTION

Head movements play an important role in gaze; the interaction between eye and head movements involves both their shared role in directing gaze and the compensatory vestibular ocular reflex. This shared role and interaction with respect to body posture and locomotion have attracted the interest of neurologists since the time of Barany, Magnus, and Dodge.

Coordinated gaze movement normally has an initial eye-in-orbit saccade onto the target followed by a synkinetic and much slower head movement. At the level of electromyographic (EMG) signal latencies, these are synchronous; but because the viscoinertial dynamics of head and neck muscles are different from the viscoelastic dynamics of eye and extraocular muscles, the saccade is over before head position has changed. The vestibular ocular reflex (VOR) generated by head acceleration drives the compensatory eye movement (CEM), eye-in-orbit, in the opposite direction so that gaze, eye-in-space, remains on target. The CEM and its VOR component are influenced by visual input and other factors that modify gain;[11,14,18,22,25,26] resultant overshoots or undershoots are corrected by later saccades. These features have been defined in monkeys and man, and some clinical studies have begun exploration of pathological changes.[1,3-7,9-13,15,16,18-20,22,24,26] Beside this classical coordinated gaze movement (type I) (FIGURE 1), other gaze patterns exist, generally determined by asynchronicity of the neural controller signals as reflected in the experimentally recorded EMGs. Sometimes head movement occurs very late (type II), at times with an anticipatory, non-VOR, compensatory eye movement (ACEM) appearing during the interval before the head movement. When the head movement occurs early (type III), eye saccades often are slowed or truncated by the interaction with the ongoing VOR. A very late eye saccade, occurring after the head movement and the VOR are completed (type IV), is a consequence of the early head movement influenced by a variety of experimental protocol conditions. These gaze patterns reflect the increased flexibility of head movements as compared with the rather stereotyped generation of eye saccades.

The methods used for head- and eye-movement recordings are well known and described elsewhere.[2,20,21,24-26]

*The authors are pleased to acknowledge support from the NCC 2-86 Cooperative Agreement, NASA-Ames Research Center.

†On leave from the University of Hamburg. Address correspondence to the Neurological University Clinic (UKE), University of Hamburg, Martinistr. 52, D-2000 Hamburg 20, Federal Republic of Germany. Supported by Deutsche Forschungsgemeinschaft, Bonn, F.R.G.

0077-8923/81/0374-0540 $01.75/0 © 1981, NYAS

Results and Discussion

Main Sequence

The dynamics of head trajectories can be parameterized to obtain the peak velocity, peak accelerations, the times of these extrema, and the duration of the movement. This parameterization is useful to show lawful relationships in the trajectory dynamics over the wide range of experimental head movements studied, and such a diagram is presented in Figure 2. The middle diagram shows the significant increase of peak velocity as a function of amplitude. The range is,

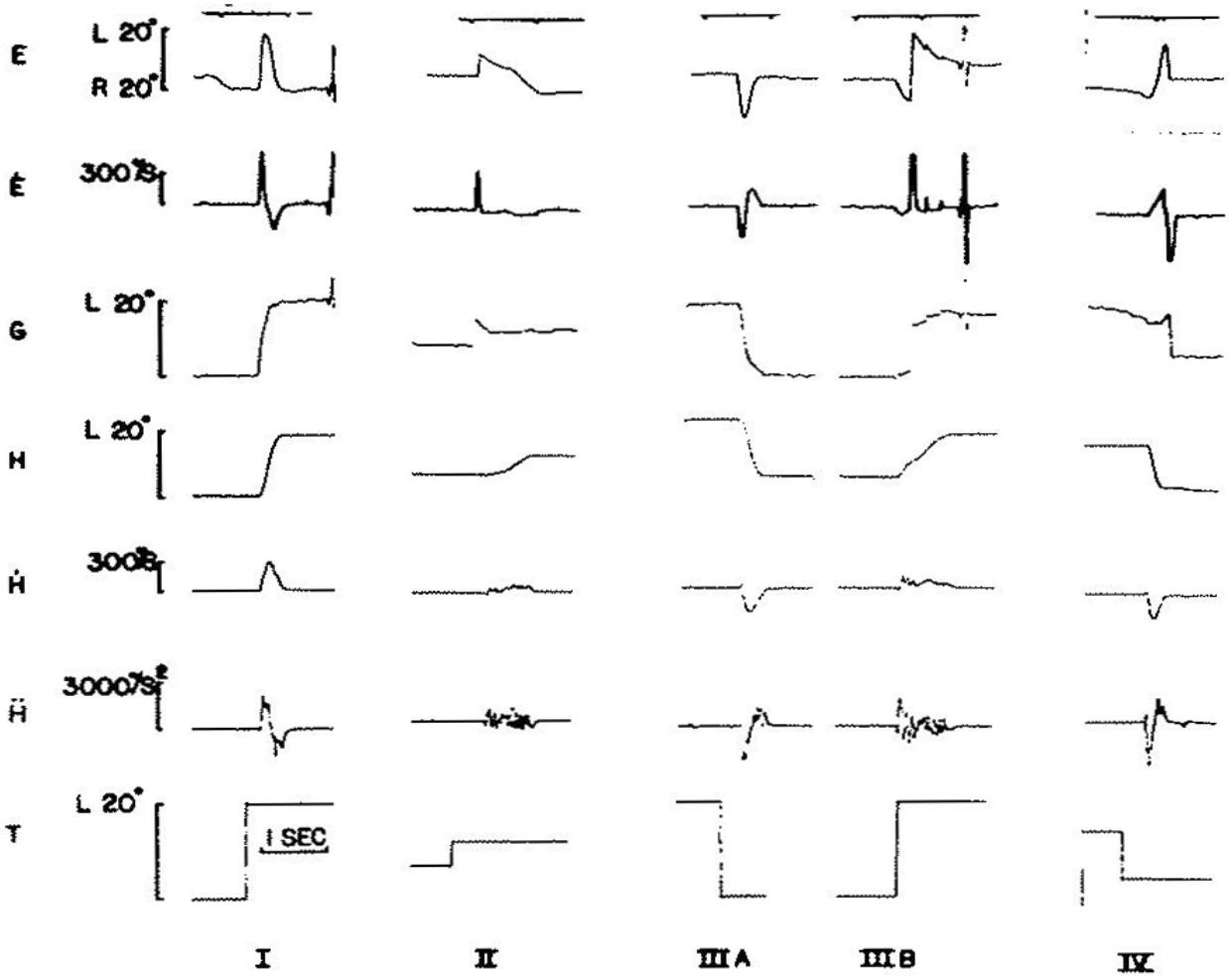

Figure 1. Coordinated gaze types. Eye position (E), eye velocity ($\dot{E}$), gaze position (G), head position (H), velocity ($\dot{H}$), and acceleration ($\ddot{H}$), and target position (T). 40° movements between left (L) and right (R).

of course, quite compressed in this log-log plot. The upper bound of the scatter of experimental results is represented by the main sequence lines; this bound is composed of the fastest movements at any given magnitude. Although velocity and acceleration increase with amplitude, the increase is not proportional, thus indicating a saturation and relative slowing of the movement. The dashed straight line in the middle diagram represents the behavior of a model for head movement simulated on a digital computer.[17,24]

A comparison between head, eye, and arm main sequence data (Figure 2.

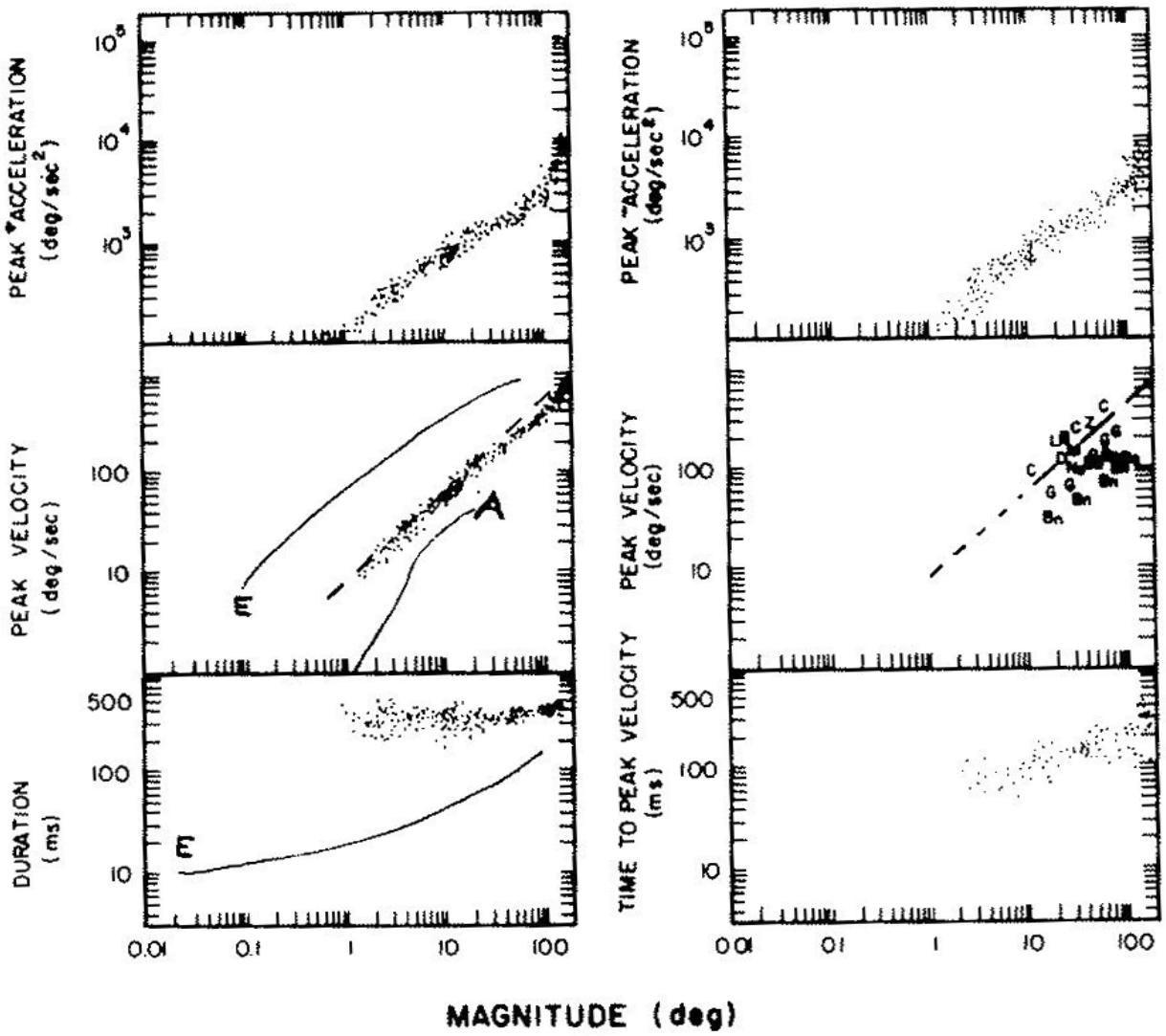

FIGURE 2. Main sequence for head movements. Over 100 fast head movements of a normal subject. Dashed line is a head-movement-model line.[24,26] Middle right shows comparative data from the literature.[2] Eye (E) and arm (A) movement main sequence data on the left show similar slopes but viscoinertially caused differing intercepts. Note the comparatively small increase of duration with large head movements.

TABLE 1) shows similar slopes but different intercepts, probably due to the different load. Also, duration increases less significantly in head than in eye movements.

Neck Muscle EMG

Neck Muscle EMG and Details of the Head-Movement Trajectory

The electromyogram is an accessible measure of the neural controller signal that governs head rotation. It thus provides useful information for interpreting and modeling dynamical details of the head-movement trajectory. Head movements are synkinetic with eye movements in gaze. Although similar to eye movements in overall properties, head movements show a contribution of stretch

TABLE 1

COMPARISON OF MAIN SEQUENCE DATA FOR EYE (E), HEAD (H), AND HEAD MODEL (HM)

	E	H	HM	E	H	HM	E	H	HM	E	H	HM	E	H	HM	E	H	HM
Magnitude (degrees)	2.5	2.5	2.5	5.0	5.0	5.0	10.0	10.0	10.0	40.0	40.0	40.0	60.0	60.0	60.0	—	140.0	140.0
Duration (msec)	24.5	260	270	28.5	270	275	37	300	295	78	320	335	110	380	385	—	412	430
v_{max} (deg/sec)	166	22.5	24	320	48	43	519	80	85	791	270	285	850	352	374	—	606	633
$t_{v_{max}}$ (msec)	—	90	105	—	95	110	—	105	115	—	125	120	—	125	130	—	150	155
a_{max} (deg/sec^2)	16000	330	310	28000	551	609	41000	994	910	73000	2100	2200	82000	3300	3250	—	6300	5900
a_{min} (deg/sec^2)	—	322	290	—	392	409	—	714	850	—	1850	1900	—	2700	2850	—	3900	4700

reflexes. There are also differences in detailed dynamic features. Electromyograms, representing samples of neurological controller signals, can be used to predict head rotations, which can be either time optimal or non–time optimal depending upon a subject's intent. A major property of neurological control signals is reciprocal innervation, and both pairs of head rotating muscles—splenius and sternocleidomastoideus muscles—demonstrate this (FIGURE 3). The (mostly biphasic and sometimes triphasic) EMG activity appears to fit the concept of optional time-optimal control in head movements, and explains the existence of dynamic overshoot in both large and small head rotations with multiple pulse control of the trajectory, seen as rapid switchings between maximum and minimum. Also demonstrated are quantitative relationships between envelopes of rectified EMG and different velocities and accelerations in head movements of the same amplitude (FIGURE 4). These relationships are lawful and quantitative on a statistical basis with averaged data. Because of the main sequence relationship (FIGURE 2), they also relate the pulse size of EMG envelopes to different head-movement amplitudes.

Kinematic factors, such as operating levels in terms of horizontal rotations, have an important influence on the tonic and phasic aspects of the EMG signal (FIGURE 4). Reciprocally innervated pairs of horizontally rotating muscles become cocontractors for vertical rotation. Correlation of detailed shapes of envelopes of rectified EMGs with detailed acceleration functions are demonstrated in several experimental paradigms. (FIGURE 4). Cocontraction, the stretch reflex, fatigue, and supraspinal influences responding to complex stimuli contribute to variance in both EMG signals and head accelerations. In addition, a number of instrumentation and biological-sampling difficulties may allow the EMG signal to be discordant with the neurological control signal for a particular movement.

Latency studies demonstrate the causal chain from target input to agonistic electromyogram (200 mseconds), to head acceleration (20 mseconds) and initial change in head position (45 mseconds), to final head position (240 mseconds) for

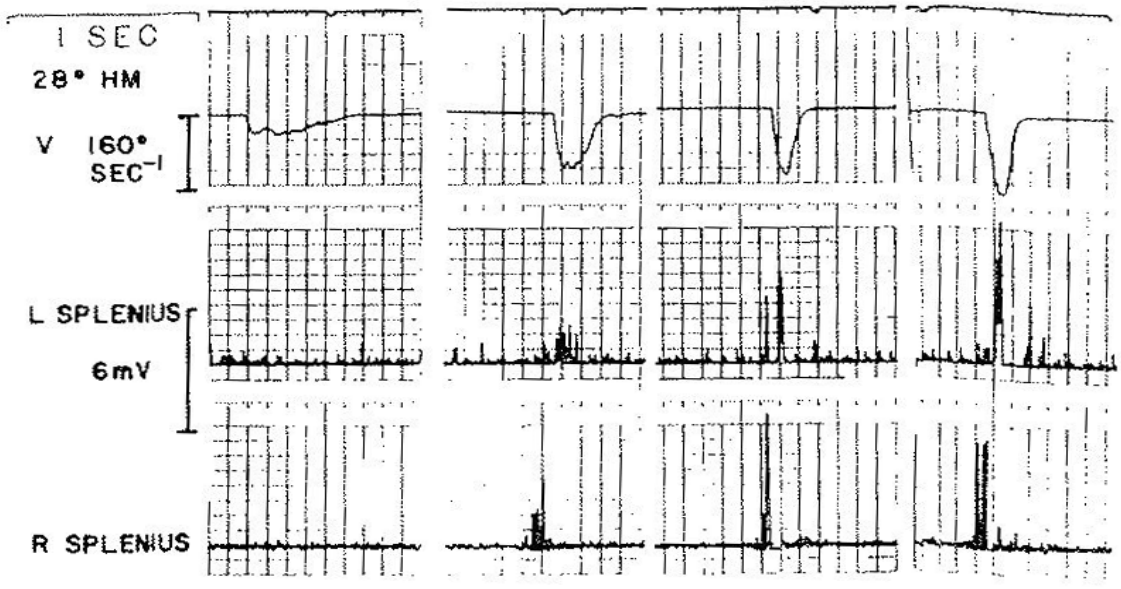

FIGURE 3. Neck-muscle EMG pulse height and pulse width as functions of head velocity (V).

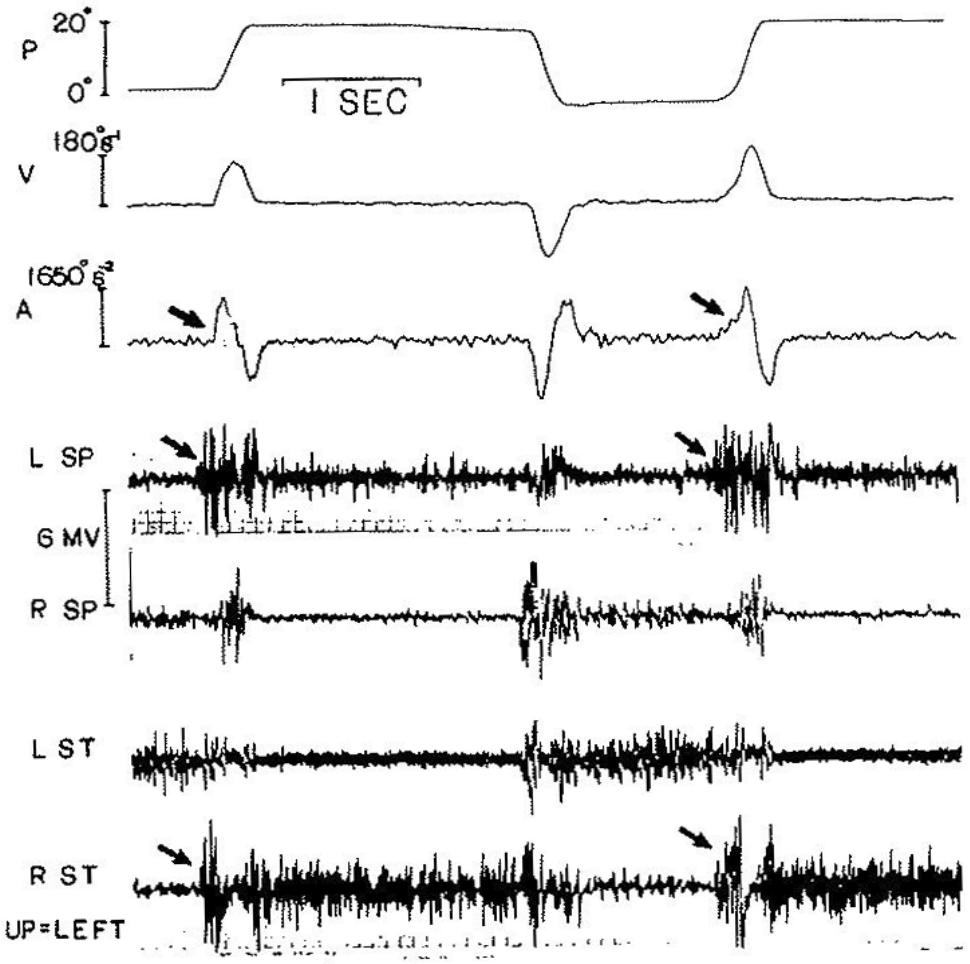

FIGURE 4. Correlation between unrectified EMG of left and right splenius (SP) and sternocleidomastoid (ST) muscles and head acceleration (*A*), velocity (*V*), and position (*P*) traces. Note abrupt onset (left arrows), contrasting with gradual onset (right arrows) of EMG and acceleration.

20° head rotations. Antagonistic EMG, obeying reciprocal innervation, begins about 70 mseconds after agonistic EMG begins. In comparison to eye movements, pulse width is less important than pulse height for the rectified EMG; this also is shown for direct or indirect modeling of head movements.[17,24,28]

Types of Head Model Accelerations

Experimentally, many different types of head-movement trajectories can be noted (FIGURE 1). One of the uses to which we put our head-movement model was to study the changes in the model that simulate different acceleration types (FIGURE 5). The four horizontal rows represent four different types arranged in decreasing order of maximum acceleration. As can be noted by looking at the right-hand column, the model fits the experimental position trajectory very well for all four types. The model also shows excellent fits to other behavioral features, such as duration, maximum velocity, maximum positive acceleration, and maximum negative acceleration. The timing behavioral parameters,

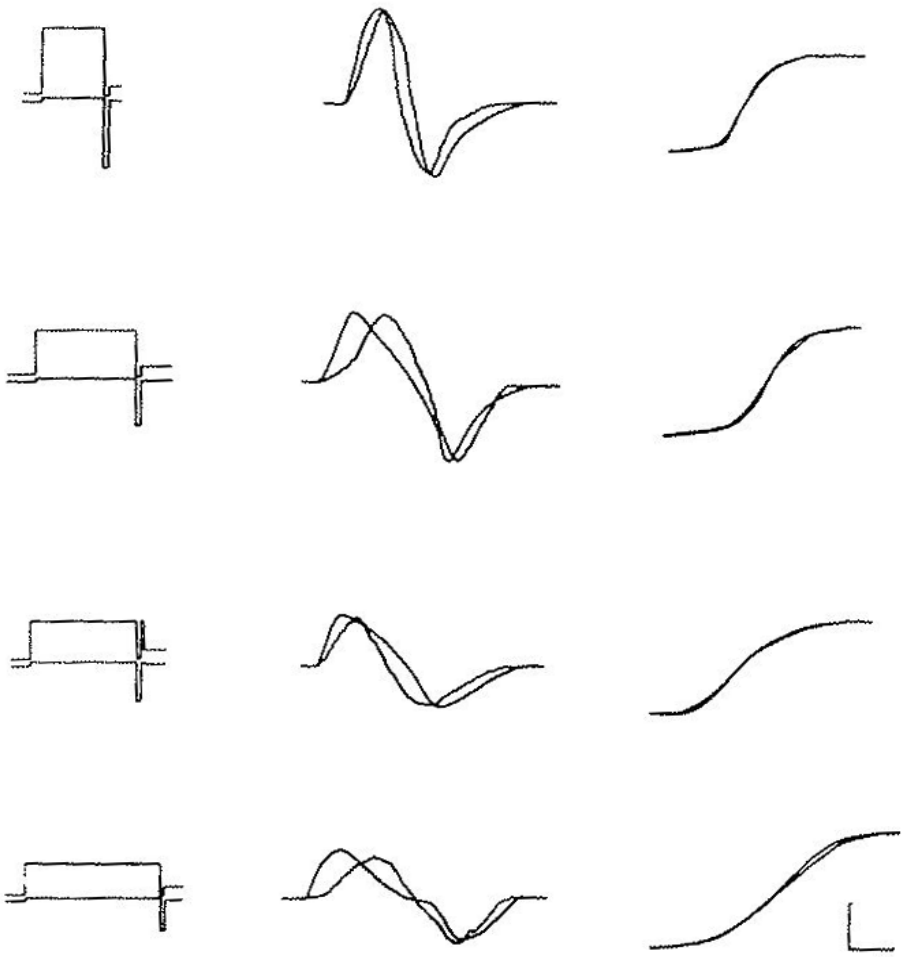

FIGURE 5. Head-movement-model fit for four acceleration types. Left: controller signal envelopes. Middle: acceleration traces (smooth lines equal model traces). Right: position. Calibration mark: abscissa, 100 mseconds; ordinate (for left, middle, and right respectively), 1,000-g force, 1,000°/second per second, 10°.

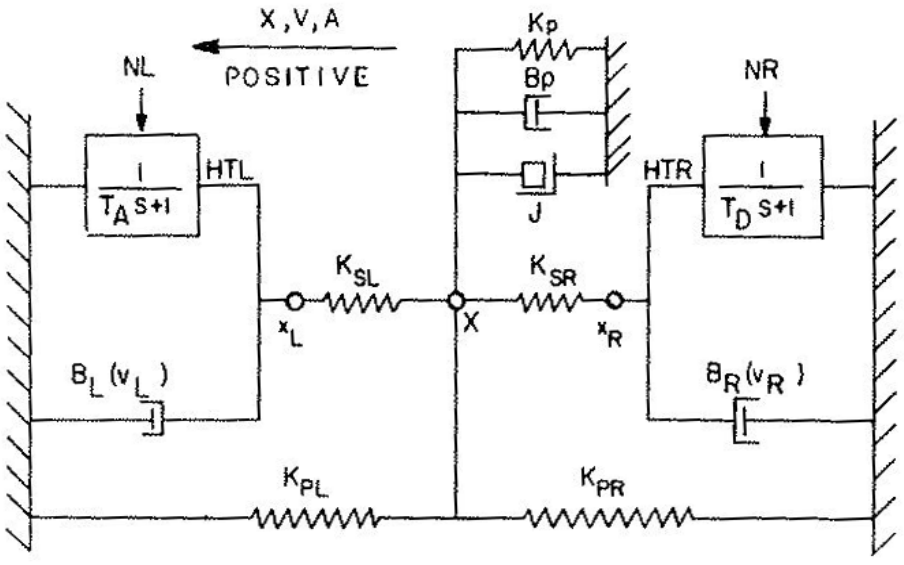

FIGURE 6. Structure of head-movement model. NL, NR: neural control signal left and right; HTL, HTR: hypothetical tensions, left and right. *X*, *V*, *A*: position, velocity, and acceleration. For other parameters, see TABLE 2.

however, were less well fitted, as can be noted in the middle column showing model and experimental acceleration trajectories.

The structure of our head-movement model is shown in FIGURE 6, and the model is compared and contrasted with the eye-movement model[17] in TABLE 2.

Latency of Eye and Head Movement in Coordinated Gaze

The classical coordinated gaze movement may be described as a saccadic eye movement followed by a head movement. Synchronously with the head movement, the compensatory eye movement returns the eye to its primary position in the orbit as an exchange of head movement for eye movement. In this way coordinated gaze obtains a first advantage from the fast eye saccade to rapidly

TABLE 2

COMPARISON OF HEAD AND EYE MODEL PARAMETERS

Definition	Parameter	Units	Eye	Head	Scaling Factor
Inertia	J	g-sec^2/deg	4.3×10^{-5}	1.8×10^{-1}	10^4
Viscosity	B	g-sec/deg	1.5×10^{-2}	2.0	10^2
Parallel Elasticity	K_p	g/deg	1.5	2.0	1
Series Elasticity	K_{sl}	g/deg	1.8	40.0	10^1
Maximum Muscle Force	F_{max}	g	100.0 (10°)	600.0 (10°) 2000.0 (40°)	10^1
Minimum Muscle Force	F_{min}	g	2.0	2.0	1
Activation Time Constant	T_a	sec	4.0×10^{-3}	5.0×10^{-2}	10^1
Deactivation Time Constant	T_d	sec	8.0×10^{-3}	5.0×10^{-2}	(10^1)

place gaze onto a target in space. It obtains a second advantage from having the eye in primary position at the end of the movement for equal ease of next moving in either direction. Although this classical description of a coordinated gaze movement has head movement occurring with a longer latency than eye movement, it must be realized that the head, being a larger mechanical object than the eyeball, requires an increased dynamical lag period in order to move. Thus we might expect that the neck EMG might begin synchronously with eye-movement EMG.

Indeed, neck EMG occurred synchronously with eye movement (FIGURE 7, left arrow), since the eye movement is almost synchronous with its own EMG (about 8 to 12 mseconds).[6,10,13] This synchronicity suggests the clarification obtained by measuring latency with respect to a controller signal and not with respect to the behavioral movement, which has its own dynamical lags. The first movement of FIGURE 7 shows a large-amplitude head movement, with the agonistic neck-muscle EMG trace (left arrow) turning on approximately 45

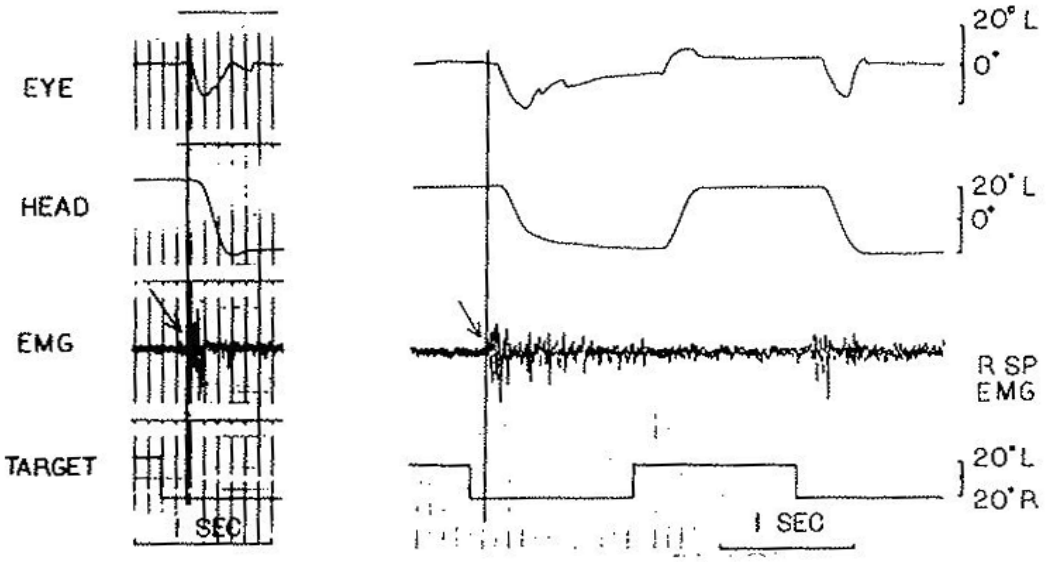

FIGURE 7. Response to a 40° target shift from right (R) to left (L) and back. Left side: unpredictable target shift. Eye movement precedes head (45 mseconds), whereas right splenius EMG (R SP) starts about 10 mseconds before initial eye-position changes. Right side: predictable target shifts. Head predicts comparatively better than does eye.

mseconds before the head movement occurs. The right experimental example shows latencies that are reduced because of prediction by about 100 mseconds. Neck EMG latency is about 50 mseconds less than latency to eye-position change; consequently, neck EMG leads eye EMG by about 40 mseconds in this predictive situation.

The dynamic lag of head movement (position, acceleration, derivative of acceleration) on a magnifying time scale with agonistic and antagonistic EMG is shown in FIGURE 8.

Gaze Latency as Function of (1) Initial Condition, (2) Amplitude, (3) Prediction, and (4) Neurological Disease Process

1. Forced or intended time-optimal coordinated gaze movements have eye-movement latencies that are shorter than head-movement latencies. The gaze-latency diagrams (FIGURE 9) demonstrate this as an offset or difference between two 45° lines. One 45° line, passing through the origin, is the line of synchronicity, that is, if all eye movements and head movements were synchronous with exactly the same latencies, then all data points would lie on this line. For 15° rapid head and eye movements, with instructions to the subject to "force" their head movements as rapidly as possible,[24] the elliptical spread of the experimental data points could be fitted by the regression line of head latency on eye latency, for which the correlation coefficient was 0.80. When standard deviations were calculated, they were approximately equal, indicating no special dependence of eye latency on head latency or of head latency on eye latency. This fitted 45° line, with a 40-msecond offset from the origin, represents a model of gaze latencies wherein head latency is 40 mseconds longer than eye latency. This of course is the dynamic head-movement lag. The fit supposes that all of the variation that is

normally seen in gaze-movement latency is a coherent covariability where head latency and eye latency vary together. This is consistent with a neural pathway between stimulus and response, part of which is shared by head and eye movement. When variability occurs in the shared part of the pathway, it is a covariability. Thus with exact covariability, all data should lie along this line; this further assumes that at some point, where there are separate paths to control eye and head movements, variation would give rise to noncoherent covariability.

When the subjects did not force their head movements in tracking the target, but rather made "natural" movements with, as might be expected, longer delays, only head-movement latency increased in this more natural situation ($r = 0.81$; FIGURE 9, upper left). Eye-movement delay seems to be stereotyped, less accessible to intent of the subject, and thus not as influenced by instructions with respect to the goal.

2. The increase of head-latency offset for a natural intent of the tracking task continued when the target amplitudes were increased from 15 to 60° (FIGURE 9, lower left). Again, latency of eye movement did not change whereas latency of head movement increased by approximately 80 mseconds ($r = 0.78$). Also it

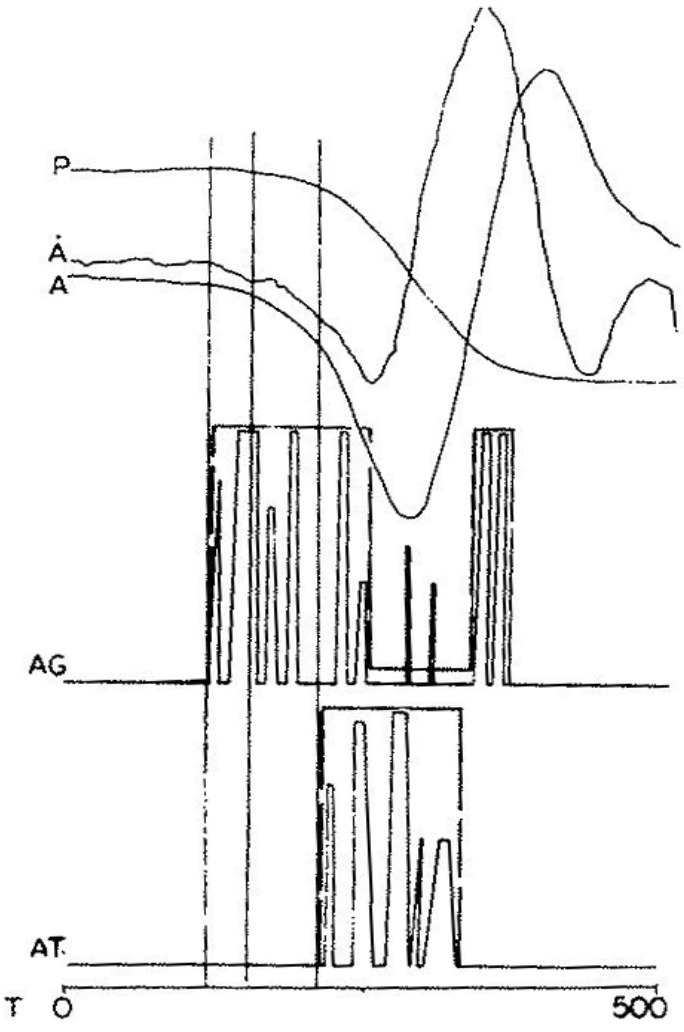

FIGURE 8. Dynamic lag in head movement. Position (P), acceleration (A), and derivative of acceleration ($\dot{A}$) show the 45-msecond position delay due to viscoinertial load following start of agonist EMG (AG). Dashed lines represent EMG pulse envelopes.

appears that amplitude for the natural task influenced latencies, that is, the larger the amplitude the longer the head latency. This somewhat smaller effect also was noted clearly by comparing the 15° forced condition with the 60° forced condition (FIGURE 9, upper left). Similarly, head latency rather than eye latency is increased in comparing these conditions.

3. Subjects greatly reduced their latency with prediction, approximately 300 mseconds (FIGURE 9, upper right). This reduction was somewhat more pronounced for head than for eye latency, but occurred to a large extent in a covarying way along the 45° line ($r = 0.95$). The slight shift towards synchrony was attributed to a somewhat more pronounced decrease for latency in head movement. When subjects, still following a predictable target, became fatigued, their predictive latencies were reduced along the covarying 45° line ($r = 0.92$).

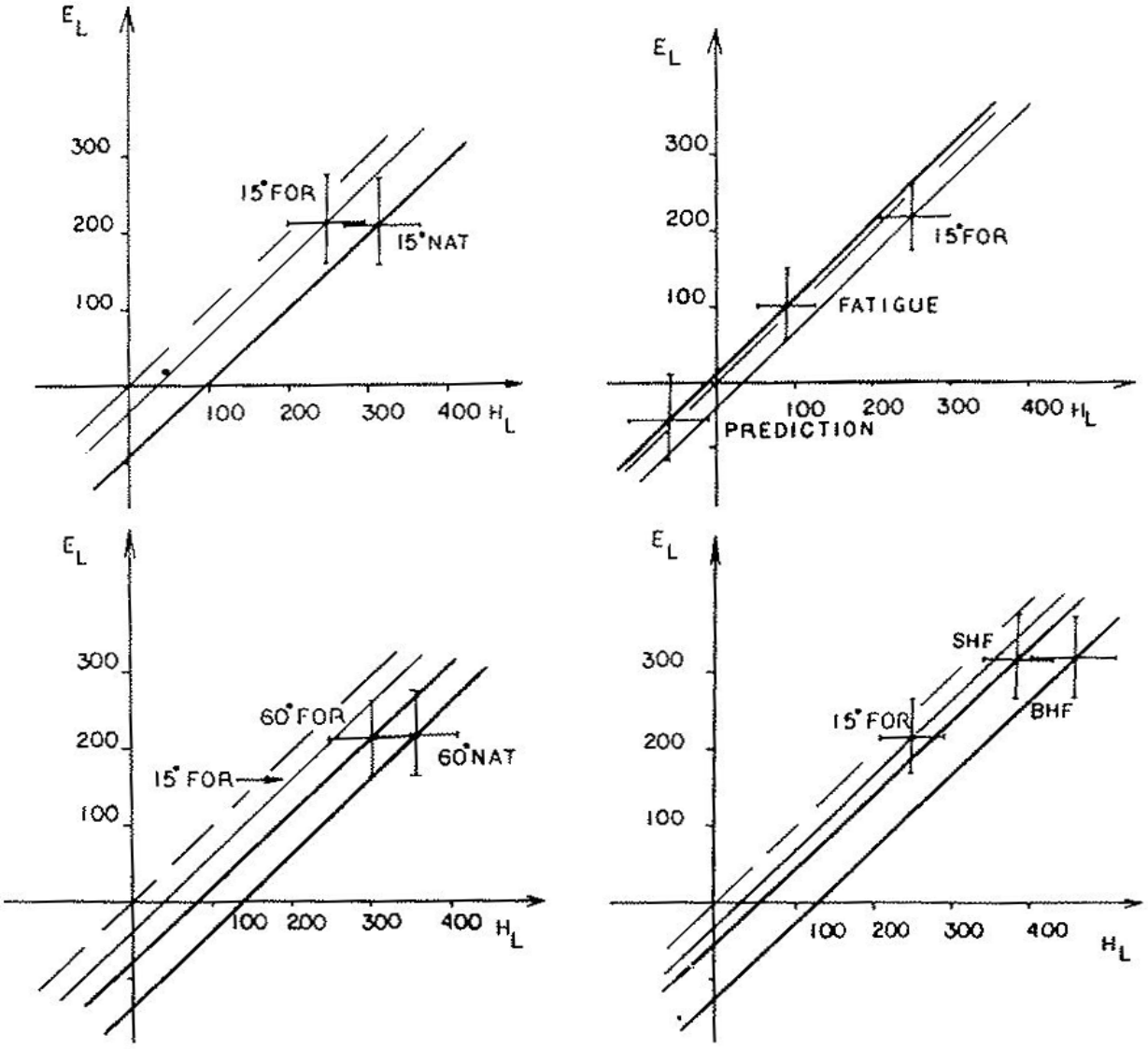

FIGURE 9. Eye- and head-latency correlations with different initial conditions in normal subjects and patients with homonymous hemianopia. 15° forced (FOR) and natural (NAT) head movements to random targets. Predictable targets (prediction) with high and low (fatigue) vigilance; patients with seeing (SHF) and blind (BHF) hemifield. Dashed line is the synchronicity line.

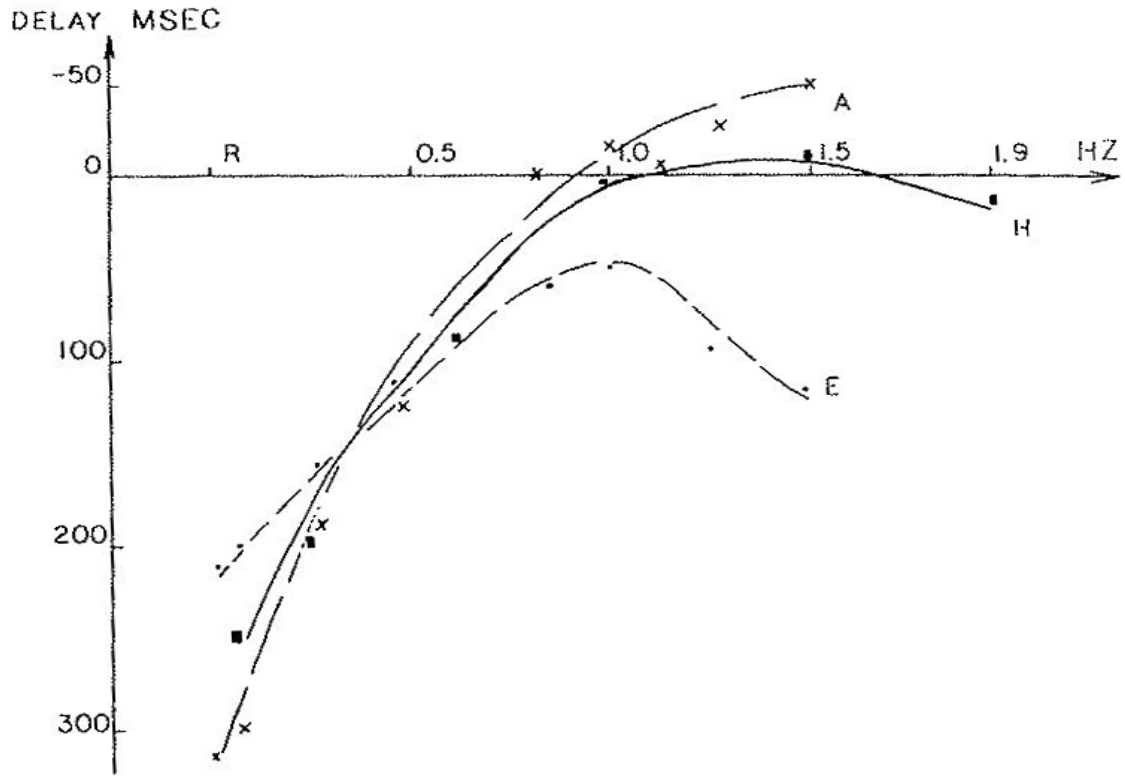

FIGURE 10. Comparison of mean head, arm, and eye delays (H, A, and E). Prediction by head and arm is superior to eye. Note the 1.5-Hz regular target oscillation, while random delay (R) is less for the eye.[21]

4. The gaze-latency diagram also was applied to a neurological disease;[18] patients with homonymous hemianopia were instructed to move their heads as fast and accurately as possible to targets of 10 and 20° amplitude. Great increase occurred in both eye-movement and head-movement latency when the subject gazed into the blind hemifield (BHF) (FIGURE 9, lower right). Quantitatively, this was in part an approximately 110-msecond increase in delay that was a covarying, or joint, delay for eye-movement latency and head-movement latency, and in part an extra delay that was noncoherent, attributed to head-movement latency only, and equal to about 120 mseconds ($r = 0.85$). When patients moved their gaze to the seeing hemifield (SHF), they showed only the covarying, approximately 110-msecond increase in latency for both eye and head movement. The center of this second latency distribution (gaze towards SHF) almost is superimposed on the normal, 15° forced line; it only has moved upwards on this 45° line (FIGURE 9, lower right).

A comparison of the differing mean delay times for head, eye, and arm movements[21] with random and predictable targets is shown in FIGURE 10.

Coordinated Gaze Types

The experimental time functions of coordinated eye and head gaze movements that have been described give an idea of the variability (FIGURE 1) and suggest a classification for clarification. To understand more deeply these gaze types and their relation to active head trajectories, it is most helpful to discuss

them in terms of a model. This model, the "gaze plane," has the advantage that eye and head movements are displayed as functions of one another with time as only an implicit function of eye and head position (FIGURE 11, right column). In the gaze-plane plot, we see the fast eye saccade occurring first (FIGURE 11, vertical arrow starting from the origin). The line pointing diagonally downwards exemplifies the CEM and the head movement occurring at the same time. Eye position is exchanged for head position, and gaze, that is, eye-in-space, remains on target throughout for the type I gaze movement. This is achieved only when the CEM gain equals unity; higher or lower gains would move gaze slightly off the target during the head trajectory. Normally this would not be a severe disturbance of the target acquisition, since the "postsaccadic snapshot"[21] already had occurred. Therefore, the target did not need to remain exactly on the fovea; after an intersaccadic interval occurred, corrective saccades could return target onto the fovea. Errors, or differences between gaze angle and target angle, are important to study because both eye and head movements are visual feedback-error-actuated movement patterns. This error function monitored continually by the subject is the important variable to be minimized as the off-foveal eccentricity of the target. Error is minimized in the type I gaze movement, where it persists only for the short eye latency and during the very rapid eye saccade, which is time optimal.[8,17] However, in the type IV gaze response, there is a much longer period before the fovea acquires the target, since the head movement finishes its trajectory following the head-movement latency (FIGURE 11, right column) before the eye even begins its saccadic trajectory. Thus the error function has a large value for the long time period of approximately 600 mseconds, which includes the 250-msecond latency of the head movement, a long head trajectory of 300 mseconds, and a subsequent fast eye saccadic trajectory of approximately 50 mseconds. This additional "excess error" present in type IV compares with the minimal error present in type I (FIGURE 11). It is represented in the gaze plane by the cross-hatched area encompassing the error during the entire period of head-eye trajectory. The time functions as well as the gaze plane demonstrate the time optimality of type I gaze pattern, considering the minimization of gaze error as the variable to be controlled. The effect of prediction is not taken into account in the gaze plane since time is only an implicit function there. Thus if the head movement of type IV were to begin so early that the late eye saccade of this type actually occurred *before* the early saccade of type I, then no excess error would occur, but rather a negative error with respect to type I.

The experimental examples (FIGURE 1) demonstrate the gaze patterns and their variability for each of the four gaze types. When we apply the gaze-plane model to the gaze types, we can abstract their basic neurological motor coordination features (FIGURE 11). The "classical" type I gaze shows, as explained, the minimal error, depending only on eye latency. An excess error does not occur. Since head acceleration can vary greatly in this type, additional errors due to nonunity CEM gain and quick-phase-like saccades occasionally take place. Type II gaze shows the delayed head-movement condition with an early gaze acquisition of the target. Typically, an anticipatory compensatory eye movement (ACEM) occurs, which does not depend on the VOR. The ACEM moves gaze off target until the head movement again brings it back onto target. The excess error shows up after the first target acquisition has occurred. Although ACEM velocity often merges indistinguishably with the subsequent CEM, its beginning (vertical line, FIGURE 11) demonstrates its important distinction from the VOR. Low-gain CEMs frequently occur that relate closely to particularly slow head velocities.[18,26]

Corrective saccades, which would delay additionally the final accurate target acquisition, are not necessary in this case.

The early head movement in type III is not due to delay in the occurrence of the eye saccade but rather to the early appearance of the head movement with its greater flexibility in predicting the target. Thus the excess error with respect to type I frequently is not nearly as great as it might be with random targets; with enough prediction, it even may be a negative quantity. Head movement often

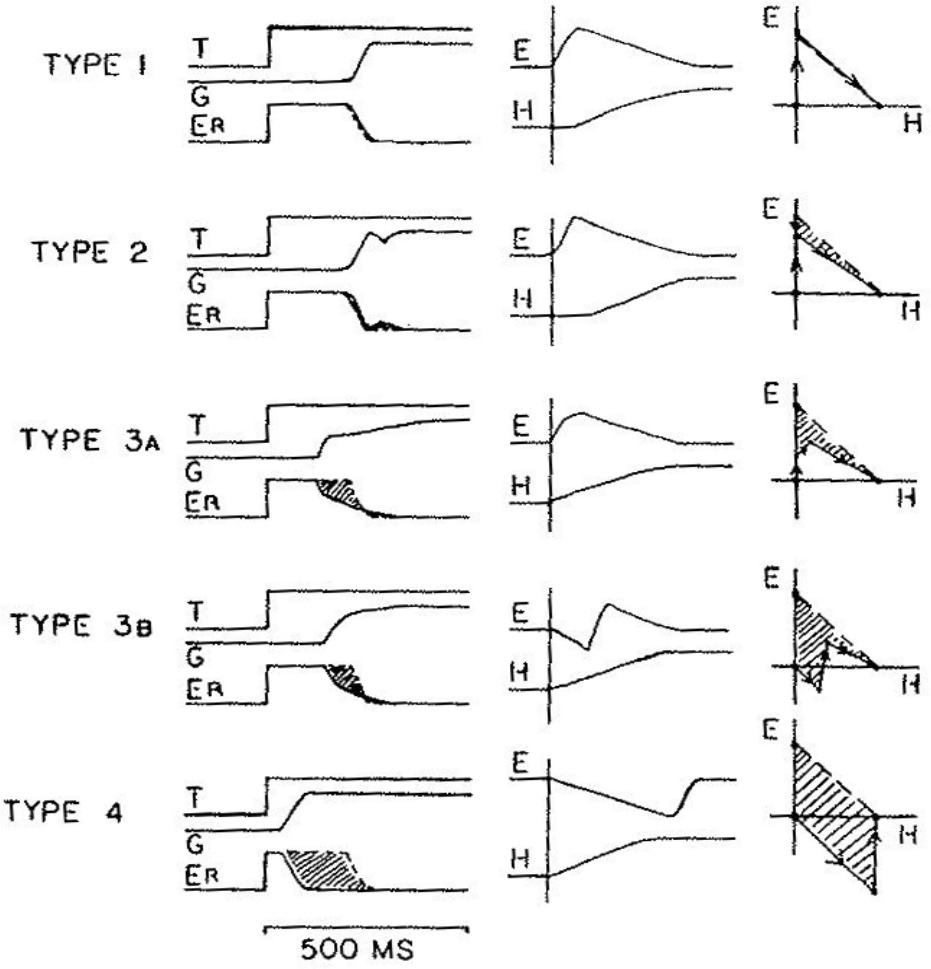

FIGURE 11. Eye and head coordinated gaze types. Left: error displays; dashed lines are excess error (ER) with respect to gaze (G) and target (T) position. Middle: eye (E) and head (H) position; vertical line indicates the relative eye and head latency. Right: gaze plane display with time as an implicit function showing excess error and eye-head interaction for the gaze types in normal subjects.

occurs early with respect to the occurrence of the eye movement, and the dynamical interactions therefore are a significant and major consideration. Two varieties are shown in the abstracted diagrams (FIGURE 11). Type IIIA shows a saccade occurring early during the head trajectory, but late enough to interact with the VOR, which slows down the saccade. When the eye saccade occurs later in the trajectory, as in type IIIB, it may be truncated due to its synchrony with a maximally active VOR occurring at peak positive head acceleration. Often this truncation is compensated for by a lowered CEM gain, which in fact may be the

result of the influence of a saccade on the ongoing VOR. Thus truncation of the saccade could be due to neuromuscular and peripheral biomechanical interactions that are dependent upon the different initial conditions of an oppositely going VOR and that influence the forces of the muscles attempting to generate the saccade.[17]‡ Another explanation for this interaction type could be an interaction of the control signals on a higher central-nervous-system level.[19] We noted also that the fast phases in type IIIB look very much like the quick phases of nystagmus, which relates type III to nystagmus generation in particular. The extreme lateness of the eye saccade in type IV provides for a great deal of excess error, especially when the very early head movement did not anticipate target movement. This excess error shows up both in the time functions and in the gaze plane. Because of the very late normal-velocity eye saccade, no peripheral interaction occurs and the eye saccade finally brings fovea and gaze onto target. However, the importance of the prediction operator is demonstrated in FIGURE 11 (lower left) showing *negative* excess error. This means that with high prediction, the very late eye saccade actually occurs earlier than the early eye saccade of type I with its minimal standard latency error.

Clinical Examples of Gaze-Plane Analysis

Clinical examples (FIGURE 12) demonstrate the variety of interactions of eye and head in gaze movements in patients with homonymous hemianopia. The upper left shows a gaze movement toward the seeing hemifield (SHH), placed in the upper-right direction in this figure (directions are plotted positively in graphs; θ_E, ordinate; θ_H, abscissa), with eye movement undershooting the target so that the right hemianopic field (represented by diagonal slashes) does not obscure the view of the target either after the first eye saccade or during head movement and CEM, or with the second eye saccade compensating or correcting for initial undershoot (small upward vertical arrow). The upper left also shows a gaze movement toward the blind homonymous hemifield (BHH), which overshoots the target on initial eye movement saccade (vertical arrow downward from the origin) so that the right hemianopic field does not obscure the view of the target. This upper-left corner of FIGURE 12 shows saccadic eye movements adaptive for safe acquisition of target. Contrariwise, maladaptive saccadic eye movements (middle left) overshoot a target in the SHH or undershoot a target in the BHH, so that view of the target is obscured by the hemianopic field.

Similarly, a change in CEM gain can be adaptive (upper middle) or maladaptive (lower middle). Unity gain has a minus 45° slope in contrast to CEM gains, greater with greater slope or lower with less slope. Corrective saccades (small vertical arrow) are required to compensate for nonunity CEM gains. The effect of the ACEM, occurring before actual head movement, is shown on the upper and middle right (FIGURE 12). On gaze to target in the SHH with accurate eye saccade, the occurrence of an adaptive ACEM places the hemianopic field away from the target and permits safe viewing of the target during head movement and CEM. A corrective saccade is necessary (small vertical upward arrow) at the end of gaze movement. A maladaptive ACEM (lower right) moves gaze off the target so that

‡KENYON, R. V., *et al.* 1980. Unequal saccades during vergence. Am. J. Optom. Physiol. Optics **57**: 586–594.

the BHH obscures view of the target. More frequently occurring clinical examples (FIGURE 12) are interpreted easily in the light of these less often occurring examples. Compensating discrepancies (left) permit safe viewing. With gaze to the SHH, an undershooting saccade (upward vertical arrow) prevents low CEM gain (downward oblique arrow) from obscuring view of the target in many instances (about 60%). Similarly, an overshooting saccade (downward vertical

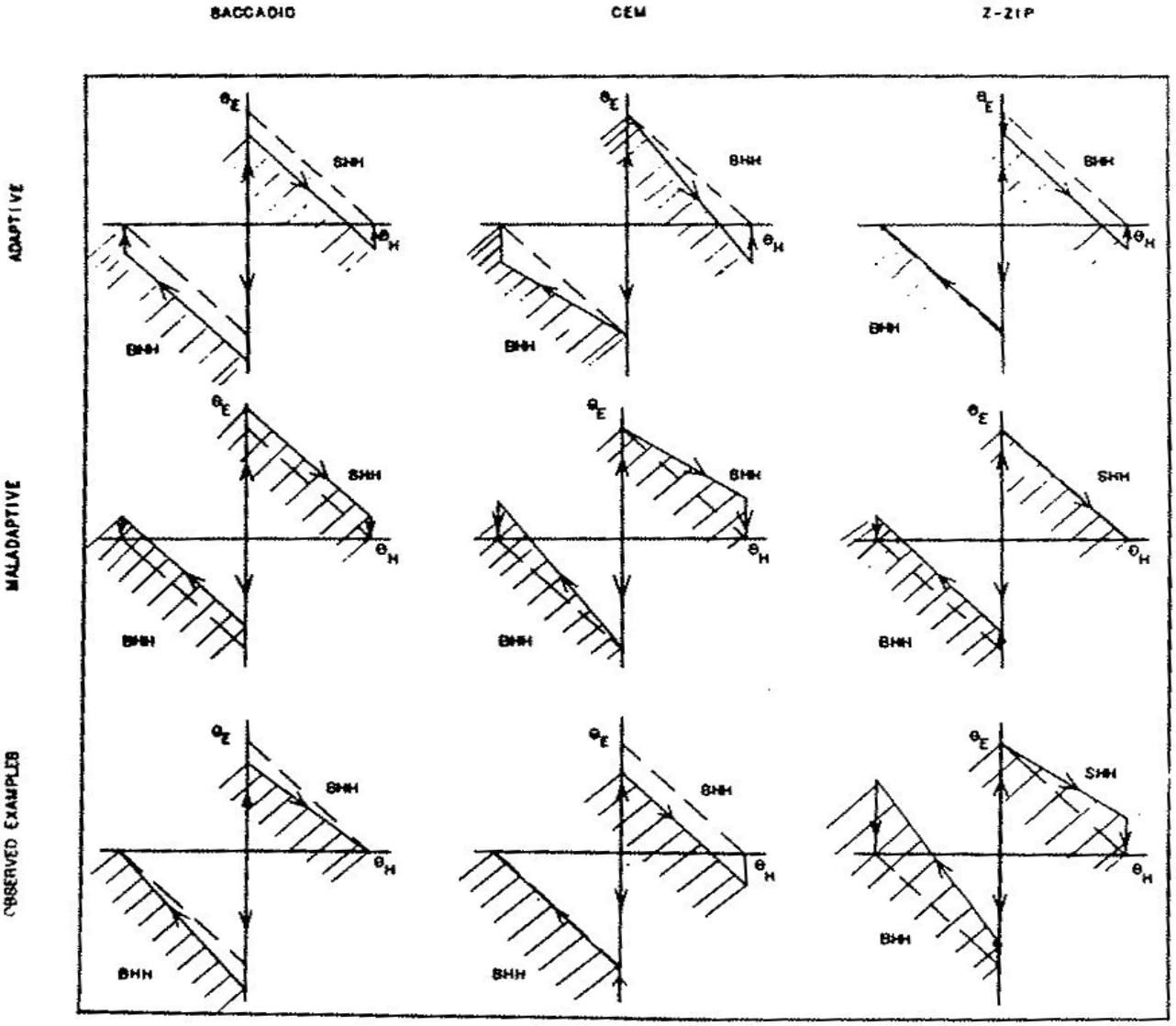

FIGURE 12. Gaze plane display for patients with homonymous hemianopia. Columns show saccadic, CEM, and ACEM (Z-ZIP) mechanisms compensating for the field defect while acquiring targets. Rows show adaptive, maladaptive, and clinically more frequent examples.

arrow) with gaze to the BHH prevents high CEM gain (upward oblique arrow) from obscuring the target in many instances (about 60%).

An especially interesting compensatory discrepancy sometimes occurs (about 25%; FIGURE 12, lowermost row, middle) when saccadic overshoot (large downward vertical arrow) with gaze to the BHH is corrected by an ACEM (small upward vertical arrow) so that the fovea is on target but without a safety margin.

A pure saccadic undershoot discrepancy also sometimes occurs (about 25%; upward vertical arrow), which permits safe target acquisition.

Maladaptive discrepancies may occur (right) with low CEM gain (downward oblique arrow) on gaze to the SHH, or with ACEM (small upward vertical arrow) and high CEM gain (upward oblique arrow). Both place target into the hemianopic field during CEM and require corrective saccades into the BHH.

Instantaneous Change of CEM Gain

A highly interesting difference in interactional modes of head and eye movements was recorded in a patient with congenital homonymous hemianopia (FIGURE 13). In our example, the target moves 20° to the right and returns after 2

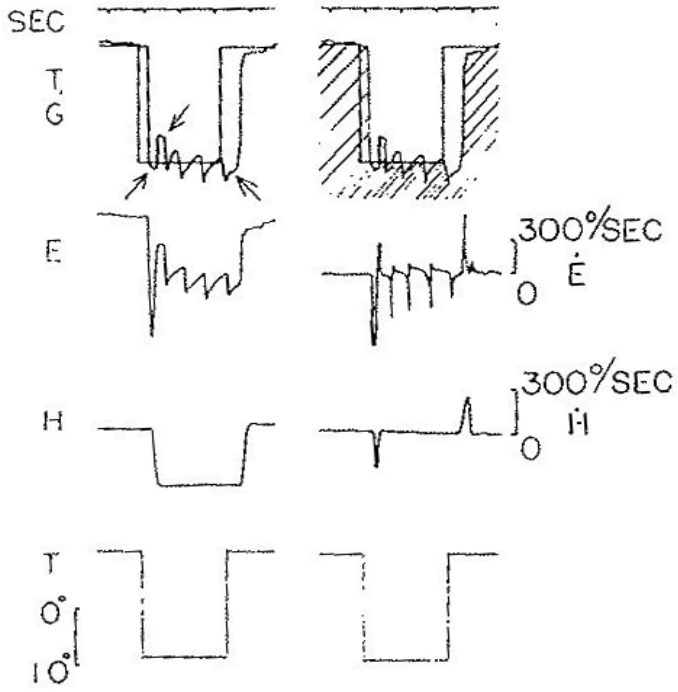

FIGURE 13. Instantaneous change of CEM gain in a patient with congenital hemianopia. Trace descriptions as in FIGURE 1. Hatched field indicates blind hemifield. Note the particularly high-gain CEM (left arrow) with gaze to right blind hemifield (down), the intersaccadic interval before correction saccades occur (middle arrow) together with continual drift, and the almost zero gaze velocity (right arrow) before a saccade and head movement with no CEM occur.

seconds—evidently not predicted in *time*, as indicated by latencies of 290 and 500 mseconds (eye) and 360 and 450 mseconds (head) to right and left. Normal values for this amplitude are 210 and 250 mseconds.[20,23,25,26] The initial 22° eye movement, obviously predicted in *amplitude*, shows small overshoot, which is typical of predictive gaze to the BHH. The fast head movement and the particularly high-gain CEM, together with a continual eye drift interrupted by corrective saccades, characteristic in this patient, bring gaze back to the target. With gaze toward the SHH, eye (10°) and head (13°) movement components place the fovea accurately onto the target. A CEM does not occur.

Here we have two completely different mechanisms or strategies of gaze movement: the first with $\theta_E = \theta_T = \theta_{CEM} = \theta_H$ permitting gaze movement to have

advantages from the speed of the first eye movement, then a continued accurate foveation, when head movement and CEM together trade θ_H for θ_E leaving gaze on target throughout, and finally eye in primary position with respect to orbit; two seconds later, a different target acquisition mode is used where θ_{eye} plus θ_{head} equals θ_{target}, with θ_{CEM} equal to zero. CEM gain clearly is suppressed or canceled; also summation with an equal and opposite smooth pursuit is not a real possibility since smooth pursuit generally would not operate at velocities of the CEM, 150°/second, and since smooth pursuit would require about 200 mseconds delay.

Variability

The CEM gain can be changed and also preset[3,5,14,15,26]—even from unity to zero within two gaze movements in this patient. Another interesting aspect is that the patient's drift is interrupted by multiple small saccades intruding on the slow movement, producing a nystagmus-type movement. A number of small saccades are seen in almost all the types, interrupted by small saccades that intrude upon the VOR reflex and appear as fragments of the fast phases of vestibular nystagmus here also. Conversely, we see in FIGURE 1 that an interrupted acceleration of the head movement appears to be a double movement and to be related to the double saccades seen in fatigued eye movements.[2] Here the interrupted fast head movement does not interfere with the vestibular ocular reflex that is generated.

What are the primary factors building the gaze types? The most important factor (TABLE 3) is the amount of prediction that the head movement undergoes so that its latency varies with respect to an EMG latency equal to the eye movement, from a late head movement (type II) to a very early head movement (type IV). We have shown that the predictability that the nervous system can use with head movements almost is equivalent to that for arm movements and is more powerful than in the eye-movement control system.[21,26] The gaze types correlate with acceleration types of head movements. The latter have been studied previously as dynamic responses and confirmed by simulations.[17,24] The type II late head movement is associated with small amplitudes and rather slow head-movement trajectories, shown by the often "fragmented" acceleration time functions. When the head movement occurs earlier than the eye saccade, we see gaze types III and IV. Both types occur quite frequently with larger amplitudes and therefore often with fast head accelerations.

Head peak positive accelerations mostly are higher than head negative accelerations and also are less "fragmented." Apparently when the head movement is large and also predicted, a highly efficient and time-optimal neural controller signal can be generated, also described in EMG studies.[6,25] With the "classical" type I gaze, both fast and slow head accelerations can be seen. The possible variability of the head trajectory is noted particularly in this type. It contrasts with the rather stereotyped eye-movement trajectory.

In concluding our observations and analyses, we see how the more intentionally governed head movement influences the eye and gaze patterns on different levels of the central nervous system. Head movement changes on a higher level with various experimental conditions (e.g. prediction), and it acts on a lower level through its variant dynamic trajectories on the VOR and therefore on the eye movement. In addition to responses in healthy subjects to various experimental conditions, patients with homonymous hemianopia demonstrate highly abnormal gaze responses

TABLE 3

INFLUENCES ON FREQUENCY OF GAZE TYPES*

Condition \ Type	I Synchronous Eye-Neck EMG (34%)†	II Late Head Movement (4%)†	III Early Head Movement (43%)†	IV Late Eye Saccade (19%)†
Amplitude (60°/15°)	0.90	0.09	3.05	2.10
Intent (forced/natural)	0.73	3.80	2.20	3.50
Predictability (high/low)	0.71	0.85	1.60	2.90
Vigilance (high/low)	0.65	5.90	1.33	0.97
Apparent Target Brightness (high/low)	1.88	1.31	0.72	0.60
Helmet Pointer (with/without)	1.04	0.55	1.27	1.11

*The table shows the four experimentally coordinated gaze types (columns) and a variety of experimental protocol conditions (rows). For each condition, a ratio is formed to indicate the influence of that condition on the probability of different gaze types.

†Mean percentage of frequency of occurrence.